

# N<sup>6</sup>-methyladenosine demethylases Alkbh5/Fto regulate cerebral ischemia-reperfusion injury

Kaiwei Xu\*, Yunchang Mo\*, Dan Li\*, Qimin Yu, Lu Wang, Feihong Lin, Chang Kong, Meita Felicia Balelang, Anqi Zhang, Sijia Chen, Qinxue Dai and Junlu Wang 

*Ther Adv Chronic Dis*

2020, Vol. 11: 1–15

DOI: 10.1177/  
2040622320916024

© The Author(s), 2020.  
Article reuse guidelines:  
sagepub.com/journals-  
permissions

## Abstract

**Background:** Although N<sup>6</sup>-methyladenosine (m<sup>6</sup>A) plays a very important role in different biological processes, its function in the brain has not been fully explored. Thus, we investigated the roles of the RNA demethylases Alkbh5/Fto in cerebral ischemia-reperfusion injury.

**Methods:** We used a rat model and primary neuronal cell culture to study the role of m<sup>6</sup>A and Alkbh5/Fto in the cerebral cortex ischemic penumbra after cerebral ischemia-reperfusion injury. We used Alkbh5-shRNA and Lv-Fto (*in vitro*) to regulate the expression of Alkbh5/Fto to study their regulation of m<sup>6</sup>A in the cerebral cortex and to study brain function after ischemia-reperfusion injury.

**Results:** We found that RNA m<sup>6</sup>A levels increased consecutive to the increase of Alkbh5 expression in both the cerebral cortex of rats after middle cerebral artery occlusion, and in primary neurons after oxygen deprivation/reoxygenation. In contrast, Fto expression decreased after these perturbations. Our results suggest that knocking down Alkbh5 can aggravate neuronal damage. This is due to the demethylation of Alkbh5 and Fto, which selectively demethylate the Bcl2 transcript, preventing Bcl2 transcript degradation and enhancing Bcl2 protein expression.

**Conclusion:** Collectively, our results demonstrate that the demethylases Alkbh5/Fto co-regulate m<sup>6</sup>A demethylation, which plays a crucial role in cerebral ischemia-reperfusion injury. The results provide novel insights into potential therapeutic mechanisms for stroke.

**Keywords:** Alkbh5, Bcl2, cerebral ischemia-reperfusion injury, Fto, m<sup>6</sup>A, MCAO, OGD/R, RNA methylation

Received: 17 August 2019; revised manuscript accepted: 18 February 2020.

## Introduction

Stroke is the leading cause of death and disability in humans.<sup>1</sup> With limited treatment options and the undesirable outcomes of current therapies, stroke remains a huge problem worldwide.<sup>2</sup> Therefore, further study of basic pathophysiological changes and possible interventions after stroke are necessary. Similar to DNA and histones, mRNAs and long non-coding RNAs can be chemically modified.<sup>3</sup> Post-transcriptional regulation of mRNAs can affect the expression of key proteins and brain functioning.<sup>4–6</sup> However, our understanding of this process is incomplete and thus requires further exploration. To that

end, we studied the regulation of epitranscriptomics after cerebral ischemia-reperfusion. In our study, we found a major, but previously unidentified, mechanism that contributes to cerebral ischemia-reperfusion injury through regulated RNA modification.

Although the mechanisms of epitranscriptomics have been studied extensively, our knowledge of their biological functions in physiological and pathological conditions remains limited. Recent studies have shown that the most abundant internal chemical modification of RNA, N<sup>6</sup>-methyladenosine (m<sup>6</sup>A), is a key regulator of mRNA stability, protein

Correspondence to:

**Qinxue Dai**  
Department of  
Anesthesiology, The  
First Affiliated Hospital  
of Wenzhou Medical  
University, Wenzhou,  
Zhejiang 325035, China  
[daiqinxue@wzhospital.cn](mailto:daiqinxue@wzhospital.cn)

**Junlu Wang**  
Department of  
Anesthesiology, The  
First Affiliated Hospital  
of Wenzhou Medical  
University, Wenzhou,  
Zhejiang 325035, China  
Wencheng County People's  
Hospital, Wenzhou,  
Zhejiang, China  
[wangjunlu973@163.com](mailto:wangjunlu973@163.com)

**Kaiwei Xu**  
**Yunchang Mo**  
**Dan Li**  
**Qimin Yu**  
**Lu Wang**  
**Feihong Lin**  
**Chang Kong**  
**Meita Felicia Balelang**  
**Anqi Zhang**  
**Sijia Chen**  
Department of  
Anesthesiology, The  
First Affiliated Hospital  
of Wenzhou Medical  
University, Wenzhou,  
Zhejiang, China

\*These authors  
contributed equally to this  
study.

expression, and several other cellular processes.<sup>3,4,7,8</sup> With advances in Me-RIP-seq technology, m<sup>6</sup>A has been the subject of extensive study.<sup>9</sup> According to studies, m<sup>6</sup>A exists mainly in the 5'-RRACH-3' (R=A or G; H = A, C or U) consensus sequence, in gene-coding regions, and in 3'UTRs.<sup>9,10</sup> Recent findings indicate that the m<sup>6</sup>A modification of mRNA is reversible and dynamically regulated by writers (methyltransferases) that catalyze the addition of m<sup>6</sup>A (such as METTL3, METTL4, METTL14, and WTAP) and erasers (demethylases) that catalyze removal of m<sup>6</sup>A (such as Fto and ALKBH5) from mRNA.<sup>11</sup> Differential expression of m<sup>6</sup>A levels regulates a variety of biological functions in mammals, such as transcript alternative splicing, nuclear RNA export, protein translation, heat shock response, cell fate determination, meiotic progression, and myocardial function.<sup>3,5,12</sup> Thus, variations in the regulatory mechanisms of m<sup>6</sup>A modification may be associated with human disease. Although dysregulated m<sup>6</sup>A is associated with various types of cancer and brain diseases,<sup>4,13</sup> the role of m<sup>6</sup>A in cerebral ischemia-reperfusion injury has not been studied.

The aim of this study is to investigate the role of m<sup>6</sup>A modification in glucose oxygen deprivation/reoxygenation (OGD/R)-treated neurons and to explore the mechanism in which m<sup>6</sup>A is involved in cerebral ischemia-reperfusion injury.

## Materials and methods

### Animals

The experimental protocol used in this study was approved by the Animal Experimental Ethics Committee of Wenzhou Medical University and was conducted according to the Animal Experiment Guide of Wenzhou Medical University, number: wyd2019-0539. Male Sprague-Dawley rats (250–300 g) were obtained from the Beijing Vital River Laboratory Animal Center, China, and were housed in a controlled environment (12h light/dark cycle; 21 ± 2°C; humidity 60–70%) for 1 week before surgery. Animals had free access to standard laboratory food and water.

### Antibodies and drugs

The following antibodies were used: anti-m<sup>6</sup>A antibody (202003, Synaptic Systems, 1:1000 for Dot blot, 1:100 for Immunofluorescence), Mouse Anti-NeuN antibody (ab104224, Abcam,

1:500) rabbit anti-ALKBH5 antibody (ab195377, Abcam, 1:1000), rabbit anti-METTL3 antibody (ab195352, Abcam, 1:1000), mouse monoclonal to FTO (ab92821, Abcam, 1:1000), BCL-2 antibody (AF6139, Affinity, 1:1000), rabbit anti-Bax antibody (ab32503, Abcam, 1:5000), Akt (4691T, Cell Signaling Technology, 1:1000), Phospho-Akt-Ser473 (4060S, Cell Signaling Technology, 1:1000), mTOR (2983T, Cell Signaling Technology, 1:1000), Phospho-mTOR-Ser2448 (5536T, Cell Signaling Technology, 1:1000), PARP (9542T, Cell Signaling Technology, 1:1000), β-Actin polyclonal antibody (AP0060, Bioworld Technology, 1:1000), Goat anti-rabbit IgG-HRP (BL003A, Biosharp Life Sciences, 1:5000), Goat anti-mouse IgG-HRP (BL001A, Biosharp Life Sciences, 1:5000), Dylight 594-donkey anti-rabbit IgG (E032421-01, Earthox, 1:500), Dylight 488-donkey anti-mouse IgG (E032211-01, Earthox, 1:500). Other reagents information is listed in Supplementary Materials.

### Cell culture

Primary cortical neurons were cultured from embryonic day 16–18 (E16–E18) rats. Briefly, embryos were removed from maternal rats anesthetized with isoflurane and euthanized by an excess of isoflurane anesthesia. The cortex was dissected in Hank's balanced salt solution and then digested with 0.125% w/v trypsin. Neurons were centrifuged (1000 × rpm, 5 min, 4°C) and resuspended in neurobasal medium containing 2% B27 serum-free supplement, 0.5% v/v penicillin/streptomycin, 0.5 mM glutamine (Neuronal standard medium). The dissociated cells were then plated at a density of 5 × 10<sup>4</sup> cells per cm<sup>2</sup> in plates pre-coated with poly-L-lysine. The culture was maintained at 37°C in a 5% v/v CO<sub>2</sub> humidified incubator. Thereafter, one-half of the medium was replaced every 3 days.

HEK293T were obtained (CRL-3216, ATCC) and cultured in DMEM containing 10% v/v fetal bovine serum (FBS), 1% v/v penicillin/streptomycin. Replace fresh medium in 2–3 days, 3–4 days cell passage.

### Glucose oxygen deprivation/reoxygenation

The neuron standard medium in the plates was initially replaced with serum-free/glucose-free DMEM medium and then transferred to an

anaerobic chamber containing a mixture of 5% CO<sub>2</sub> and 95% N<sub>2</sub> at 37°C for 3 h. During reperfusion, the cells were then returned to an oxygen-containing incubator (95% air and 5% CO<sub>2</sub>) for 24 h with normal neuron standard medium.

#### *Middle cerebral artery occlusion*

Intraluminal filament technique was used to induce focal cerebral ischemia, as previously described.<sup>23</sup> Briefly, animals were anesthetized with 10% chloral hydrate (350 mg/kg) intraperitoneally. The nylon thread (2636A4/2838A4, Bei Jing Cinontech Co. Ltd) was inserted through the external carotid artery, and the blood flow was blocked by the adjustment of the nylon thread into the common carotid artery to the internal carotid artery and finally occluded the middle cerebral artery. Reperfusion was achieved by withdrawing the nylon thread after 1.5 h of ischemia, and the wound was stitched up. Regional cerebral blood flow was monitored using a transcranial laser Doppler flowmeter (PeriFlux 5000; Perimed AB, Sweden). MCAO was considered sufficient if local cerebral blood flow decreased to 20% of pre-ischemia; if not, animals were excluded.

#### *RNA m<sup>6</sup>A dot blot*

The dot blot was performed as described above and some minor changes were made.<sup>8</sup> Total RNA was isolated using TRIzol (Invitrogen, 15596018) according to the manufacturer's instructions, and RNA quality was analyzed using DeNovix. RNA (100 ng) was spotted onto a nylon membrane (RPN303B, GE Healthcare Life Sciences). The membrane was then UV-crosslinked and blocked in TBST [0.1% Tween 20 plus TBS (50 mM Tris-Cl, pH 7.5, 150 mM NaCl)] containing 5% milk for 1 h. Rabbit anti-m<sup>6</sup>A antibody was incubated overnight with the membrane (4°C). After washing three times with TBST, Goat anti-rabbit IgG-HRP was incubated with the membrane for 1 h at room temperature. The TBST was washed three times and the reaction was observed using an ECL chemiluminescent reagent. The same amount of RNA was spotted on the membrane, stained with 0.02% methylene blue in 0.3 M sodium acetate (pH 5.2) for 2 h, and washed with ribonuclease-free water for 5 h.

#### *Immunohistochemistry*

The brain was removed 24 h post-reperfusion. Rats were perfused with 4% paraformaldehyde

through the left ventricle. Paraffin sections (3.5 mm thick) were deparaffinized and immersed in 3% hydrogen peroxide for 10 min to block endogenous peroxidase activity. The sections were boiled with 10 mmol/L citrate buffer for antigen retrieval and cooled to room temperature by natural cooling. Sections were blocked with 5% bovine serum albumin (BSA) in phosphate buffered saline (PBS) for 1 h at room temperature, and sections were incubated overnight with 1% BSA diluted Anti-ALKBH5 antibody. The next day, sections were washed three times with PBS, and horseradish peroxidase (HRP)-conjugated secondary antibody (PV-6001, ZSGB-BIO) was added, incubated for 30 min at 37°C, then washed 3 times with PBS. DAB coloring solution (ZLI-9018, ZSGB-BIO) was then added, and stop color reaction with double distilled water in time. Hematoxylin was counter-dyed for 3–5 min, washed for 5 s and sealed with a neutral resin. We analyzed the results using Image-Pro Plus.

#### *Immunofluorescence*

The brain was removed 72 h post-reperfusion. Rats were perfused with 4% paraformaldehyde through the left ventricle. Paraffin sections (3.5 mm thick) were deparaffinized and immersed in 3% hydrogen peroxide for 10 min to block endogenous peroxidase activity. The sections were boiled with 10 mmol/L citrate buffer for antigen retrieval and cooled to room temperature by natural cooling. Sections were blocked with 5% BSA in PBS for 1 h at room temperature and sections were incubated overnight with 1% BSA diluted rabbit anti-m<sup>6</sup>A antibody and mouse Anti-NeuN antibody. After washing three times with PBS, a fluorescent secondary antibody was added for 1 h, and, after washing 3 times with PBS, the plate was sealed with 4'-diamidino-2-phenylindole (DAPI). Fluorescence images were obtained using an OLYMPUS BX51 fluorescence microscope. Gain, threshold, and black levels did not change during the respective experiments. All image analyses were performed under experimental conditions.

#### *Immunocytochemistry*

Immunofluorescence staining was performed in cultured neurons of DIV14. Briefly, neurons were fixed by PBS containing 4% paraformaldehyde for 15 min and permeabilized with 0.2% Triton-100 for 10 min. Neurons were blocked with 5% BSA

in PBS for 1 h at room temperature and then incubated overnight with primary antibody in PBS containing 1% BSA. After washing three times with PBS, a fluorescent secondary antibody was added for 1 h, and, after washing 3 times with PBS, the plate was sealed with DAPI. Fluorescence images were obtained using an OLYMPUS BX51 fluorescence microscope. Gain, threshold, and black levels did not change during the respective experiments. All image analyses were performed under experimental conditions.

#### Quantitative real-time polymerase chain reaction

Total RNA was extracted using Trizol reagent. cDNA was generated using 1 µg of RNA from each sample using a RevertAid First Strand cDNA Synthesis Kit (K1622, Thermo Scientific) according to the manufacturer's protocol. Real-time PCR was performed using SYBR® Premix Ex TaqII Kit (RR820A, Takara) of Applied Biosystems QuantStudio 5 Real-Time PCR Systems. Amplification products were quantified using the  $2^{-\Delta\Delta CT}$  method. The relative expression of the protein of interest was normalized to the expression of  $\beta$ -actin (B661202-0001, Sangon Biotech). All primers used in this study were synthesized chemically by Sangon Biotech (Shanghai) Co., Ltd, and are detailed in Supplementary Materials.

#### Western blotting

Protein was extracted using RIPA lysis buffer and protein concentration was determined using the BCA Protein Assay Kit. Equal amounts of protein were separated by 10% SDS-PAGE and transferred to a polyvinylidene difluoride (PVDF) membrane (1620177, Bio-Rad). The membrane was blocked with 5% skim milk in TBST for 1 h at room temperature and incubated with primary antibody overnight at 4°C. After washing three times with TBST, it was then incubated with a suitable horseradish peroxidase (HRP)-conjugated secondary antibody for 1 h at room temperature and washed three times with TBST. The reaction was observed using an ECL chemiluminescent reagent. The intensity of the blot was quantified using Image lab.

#### Generation of Fto expression constructs

The Fto cDNA was cloned from previously obtained Rat cDNA using PrimeSTAR Max

DNA Polymerase (R045Q, Takara) using the following primers and conditions: (forward 5' CGTCTAGAATGAAGCGCGTCCAGACCG3', reverse 5'CGGAATTCCTAGGATCTTGCTTCCAGAAGCTGG3'); 25 cycles at 98°C (10s), 60°C (15s), 72°C (30s). PCR products were subsequently digested with *EcoRI* and *XbaI* and purified by AxyPrep DNA Gel Extraction Kit (AP-GX-50, Axygen) and ligated into similarly digested pCDH-EF-FHC vector. pCDH-EF-FHC-Fto was propagated and sequenced for inserting verification.

#### Lentivirus production

To generate lentiviruses for transduction,  $6 \times 10^6$  293T cells were seeded into 10 cm<sup>2</sup> culture dishes with 10 mL complete medium and grown to 60–80% confluence. 293T cells were co-transfected with pRev (0.5 µg), pMDL (1 µg), pVSVG (2 µg) (the lentiviral envelope and packaging plasmids were kindly provided by Jianjing Lin) and pCDH-EF-FHC-Fto (4 µg) expression vectors using polyethylenimine. Fresh medium was replaced after 16 h of transfection, and the culture continued for 24/48 h to harvest the virus-containing medium, which was filtered through a 0.45 µm syringe filter and stored at –80°C until use.

#### Lentivirus infection

DIV7 cultured cortical neurons were infected with a lentivirus carrying GV112-Alkbh5-shRNA (Alkbh5-shRNA) (Shanghai Genechem Co., Ltd) according to the vendor's protocol to knock down Alkbh5. Lentivirus expressing GV112-scramble-shRNA (Ctrl-shRNA) was used as a control. Target sequences for Alkbh5 and Ctrl siRNAs are siRNA1: GCGCAGTCATCAACGACTA, siRNA2: GCC TCAGGACATCAAAGAA, and Ctrl: TTCT CCGAACGTGTACAGT. DIV10 cultured cortical neurons were infected with lentivirus carrying pCDH-EF-FHC-Fto (Lv-Fto) to overexpress Fto. A lentivirus expressing pCDH-EF-FHC (Lv-Ctrl) (Addgene plasmid # 64874<sup>26</sup>) was used as a control. These were subsequently used for Western blotting or flow cytometry.

#### Cycloleucine or betaine treatment

Neurons were cultured *in vitro* for neuron standard medium supplemented with cycloleucine (CL) [A1063, TCI (Shanghai) Chemical Industry Development Co., Ltd.] (10mM, 20mM, 40mM)

and betaine (61962, Sigma) (4mM, 8mM, 16mM) from 24h before OGD to the end of the experiment. According to a previously published article,<sup>14</sup> the optimal concentration was determined and then used in subsequent experiments.

#### *Apoptosis analysis*

The neurons were processed according to the experimental requirements, and the supernatant and PBS washing solution were collected, trypsinized for 5 min, 10% v/v FBS was used to terminate the digestion, and the cells were harvested. Cell death assays were performed using FITC Annexin V Apoptosis Detection Kit I (556419, BD). Briefly, the cells were resuspended in 300  $\mu$ l of 1X Binding Buffer, 5  $\mu$ l of FITC Annexin V was added and mixed, then incubated at room temperature for 15 min in the dark. Then, 5  $\mu$ l of propidium iodide (PI) was added, mixed, and incubated at room temperature in the dark for 5 min. Finally, 200  $\mu$ l of 1X binding buffer was added to each tube. Samples were analyzed on CytoFLEX LX flow cytometers (Beckman Coulter, USA) and all flow cytometers operations were performed by laboratory professionals. CytExpert V2.3 software was used to calculate the percentage of cells positive for FITC Annexin V and PI.

#### *Cell counting Kit-8 assay*

Primary cortical neurons were extracted as described above, and a single cell suspension was prepared using neuron standard medium;  $2 \times 10^4$  cells per well were seeded into 96-well plates at a volume of 100  $\mu$ l per well. The cells were cultured under normal culture conditions. After 14 days of culture, the OGD/R model was used, and 10  $\mu$ l of CCK8 solution was added per well, and incubation was continued for 2h. The wavelength of 450nm was selected, and the light absorption value of each well was measured on a microplate reader, and the results were recorded.

#### *Hoechst 33342/PI double stain*

Neurons were processed according to experimental requirements and stained according to the manufacturer's instructions. Briefly, the supernatant was removed, washed once with PBS, 1 ml of cell staining buffer was added, 5  $\mu$ l of Hoechst staining solution was added, incubated at 4°C for 15 min, 5  $\mu$ l of PI staining solution was added, and incubated at 4°C for 5 min. The cells were

washed once with PBS, and the results were observed and recorded under a fluorescence microscope.

#### *Statistical analysis*

GraphPad Prism (version 6.01, Graph-Pad Software Inc.) was used for data display and statistical analysis. We did not predetermine the sample size. Data were showed as mean  $\pm$  SEM. Differences between two or more groups were analyzed by Student's *t* test and ANOVA, respectively. *P* values < 0.05 were considered statistically significant.

## Results

#### *Increased m<sup>6</sup>A expression after OGD/R and MCAO*

To investigate whether m<sup>6</sup>A modification is involved in ischemia/reperfusion (I/R)-induced brain tissue injury, middle cerebral artery occlusion (MCAO) was performed in Sprague-Dawley rats. The level of m<sup>6</sup>A modification was measured by m<sup>6</sup>A dot blot. The level of m<sup>6</sup>A modification was significantly increased in the brain after MCAO (Figure 1A). To further confirm the change in the m<sup>6</sup>A modification level, immunofluorescence staining was performed on MCAO-treated rat brain tissue. We observed a similar significant increase in the m<sup>6</sup>A modification level after MCAO treatment that was localized mainly in neurons (Figure 1B). We therefore measured m<sup>6</sup>A modification levels within *in vitro* primary cortical neurons after OGD/R-exposure. Consistent with the brain tissue of rats subjected to MCAO treatment, the levels of neuronal m<sup>6</sup>A modification were significantly increased after OGD/R (Figure 1C). We also performed immunofluorescence staining on primary neurons. A significant increase in m<sup>6</sup>A levels after OGD/R treatment was observed (Figure 1D). These results indicate that m<sup>6</sup>A levels are dynamically regulated in both primary neurons after OGD/R treatment and rat brain tissue after MCAO treatment.

#### *OGD/R and MCAO induce Fto upregulation in neurons and cerebral cortex*

To determine the regulators responsible factors for the increase in m<sup>6</sup>A levels after I/R, we examined previously identified proteins that affect m<sup>6</sup>A methylation (writers such as Mettl3 and Mettl14) and demethylation (erasers such as Fto and

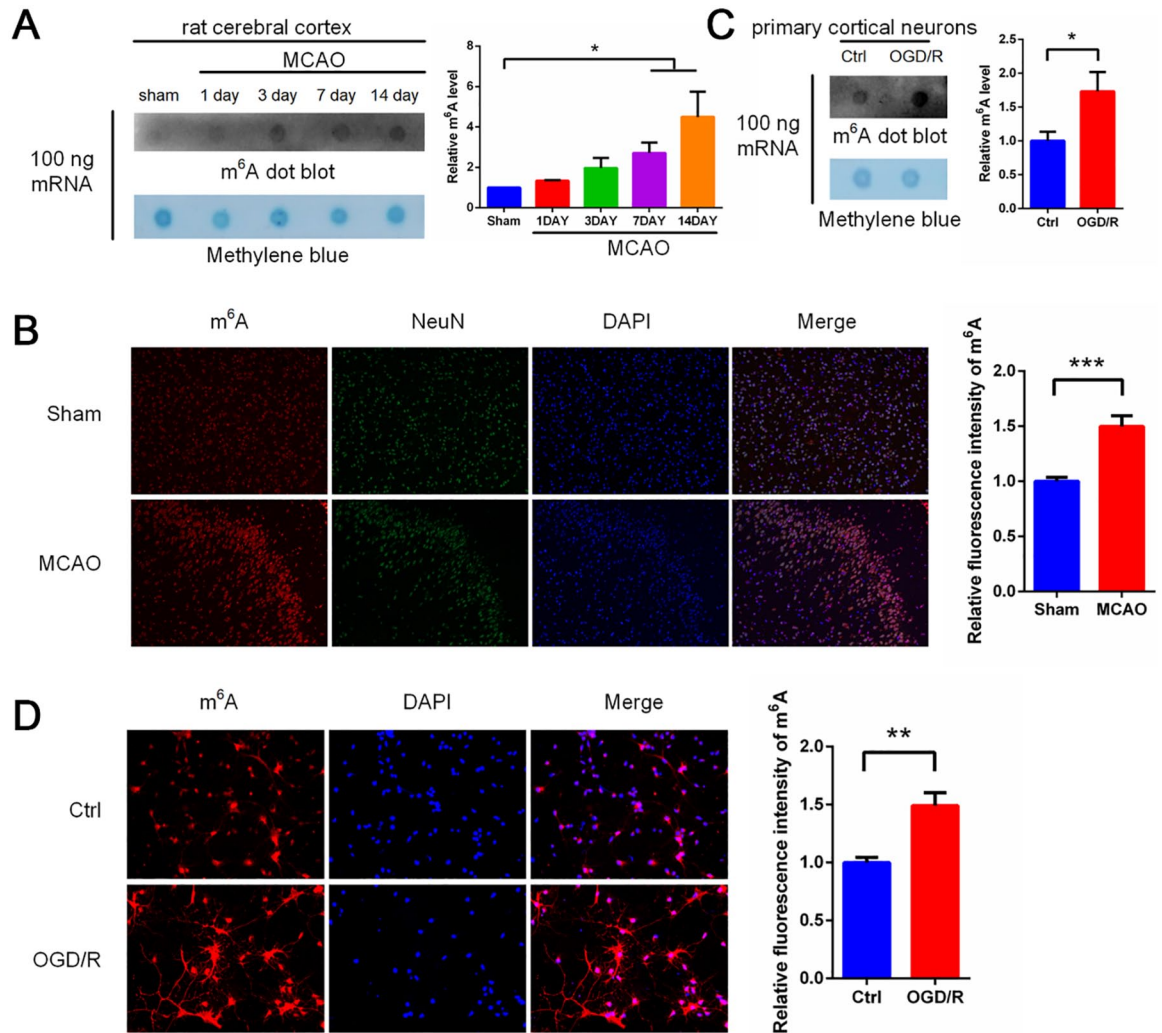


**Figure 1.** MCAO and OGD/R induces increased levels of m<sup>6</sup>A RNA modification in rat cerebral cortex and primary cerebral cortical neurons, respectively. (A) RNA dot blot analysis of m<sup>6</sup>A levels in MCAO-treated rat cerebral cortex (top left panel). Methylene blue staining was used as a loading control (bottom left panel). Quantification of RNA dots is shown (right panel) [mean ± SEM; *n* = 3; \**p* < 0.05 versus sham]. (B) Immunofluorescence results of MCAO-treated rat cerebral cortex: red staining represents m<sup>6</sup>A modification, green staining represents NeuN protein, and blue staining represents DAPI. The m<sup>6</sup>A modification were quantified by IOD values (mean ± SEM; *n* = 6; \*\*\**p* < 0.001 versus sham). (C) RNA dot blot analysis of m<sup>6</sup>A levels in primary cerebral cortical neurons treated with OGD/R (top left panel). Methylene blue staining was used as a loading control (bottom left panel). Quantification of RNA dots was shown (right panel) [mean ± SEM; *n* = 9; \**p* < 0.05 versus Ctrl]. (D) Immunofluorescence results of primary cerebral cortical neurons treated with OGD/R: red staining represents m<sup>6</sup>A modification and blue staining represents DAPI, and quantification of m<sup>6</sup>A modification was shown [mean ± SEM; *n* = 4; \*\**p* < 0.01 versus Ctrl].

Ctrl, control; DAPI, 4',6'-diamidino-2-phenylindole; m<sup>6</sup>A, N<sup>6</sup>-methyladenosine; IOD integrated optical density; MCAO, middle cerebral artery occlusion; OGD/R, glucose oxygen deprivation/reoxygenation; SEM, standard error of the mean.

Alkbh5) levels in primary neurons and rat brain tissue. Our Western blot and quantitative reverse transcriptase-polymerase chain reaction (qRT-PCR) results show that Fto mRNA and protein levels were decreased significantly both in rat brain

tissue after MCAO and in primary neurons following OGD/R (Figure 2A–C). In addition, our histochemical results show that MCAO treatment significantly reduced the number of Fto-positive cells in the ischemic penumbra of rat brain tissue

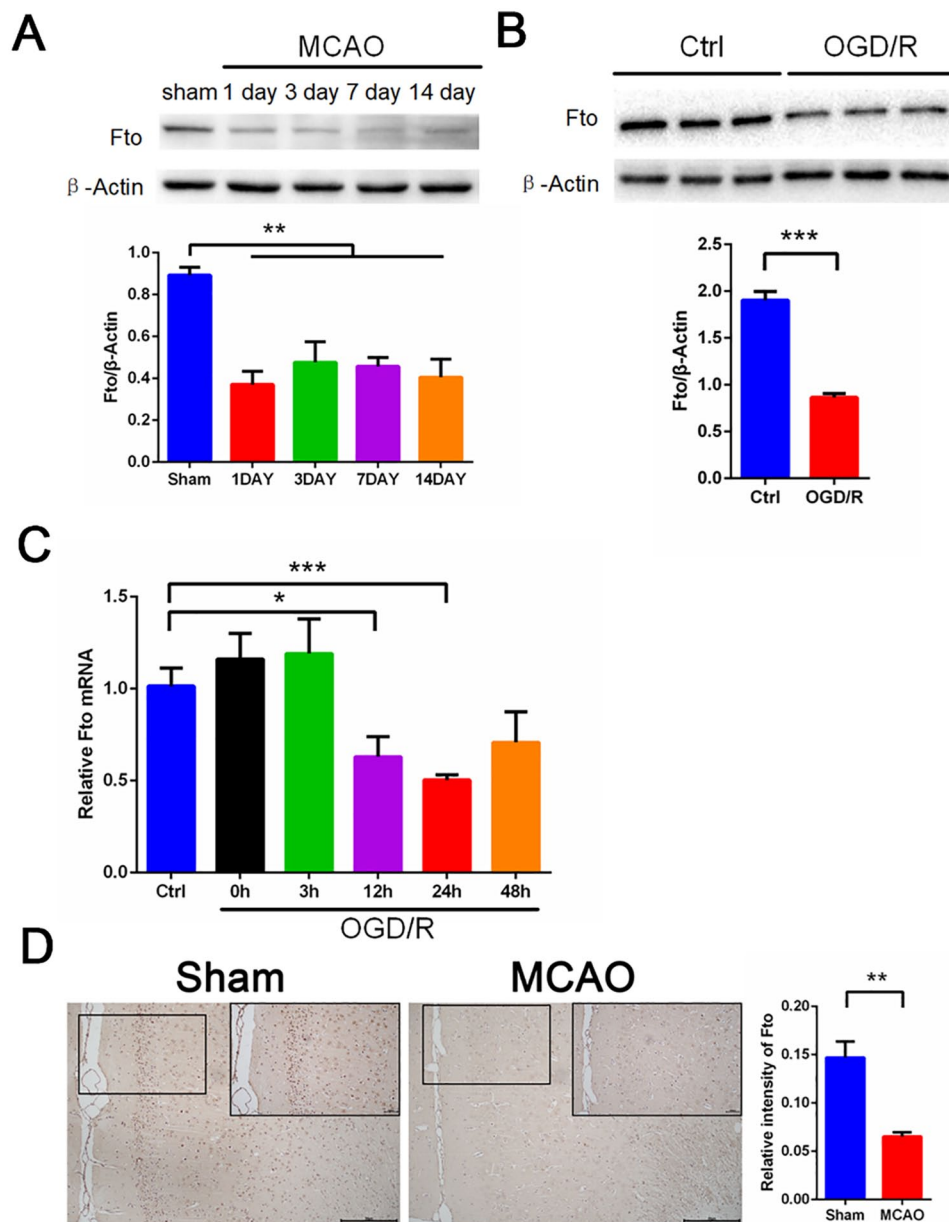


**Figure 2.** MCAO and OGD/R induces decreased levels of Fto both in rat cerebral cortex and primary cerebral cortical neurons. (A) Representative images of Western blots of MCAO-treated rat cerebral cortex. Fto levels were determined by Western blot (mean  $\pm$  SEM;  $n=3$ ;  $**p < 0.01$  versus sham). (B) Representative images of Western blots of OGD/R treated primary neurons. Fto levels were determined by Western blotting (mean  $\pm$  SEM;  $n \geq 3$ ;  $***p < 0.001$  versus Ctrl). (C) qRT-PCR images of OGD/R treated primary neurons. Fto levels were analyzed by qRT-PCR. (mean  $\pm$  SEM;  $n \geq 3$ ;  $*p < 0.05$ ,  $***p < 0.001$  versus Ctrl). (D) Immunohistochemical results of Fto in rat cerebral cortex in two indicator groups: tawny staining for Fto protein and light blue staining for hematoxylin. Scale bar = 100  $\mu$ m, and the small picture scale bar = 2000  $\mu$ m. Quantification of Fto was shown (mean  $\pm$  SEM;  $n=3$ ;  $**p < 0.01$  versus Sham). Ctrl, control; MCAO, middle cerebral artery occlusion; OGD/R, glucose oxygen deprivation/reoxygenation; qRT-PCR, quantitative reverse transcriptase-polymerase chain reaction; SEM, standard error of the mean.

(Figure 2D). Interestingly, Western blot and qRT-PCR data shows that Alkbh5 expression levels were significantly increased in rat brain tissue after

MCAO and in primary neurons following OGD/R (Figure 3A and Figure S1A–C). Similarly, we observed a significantly increased number of

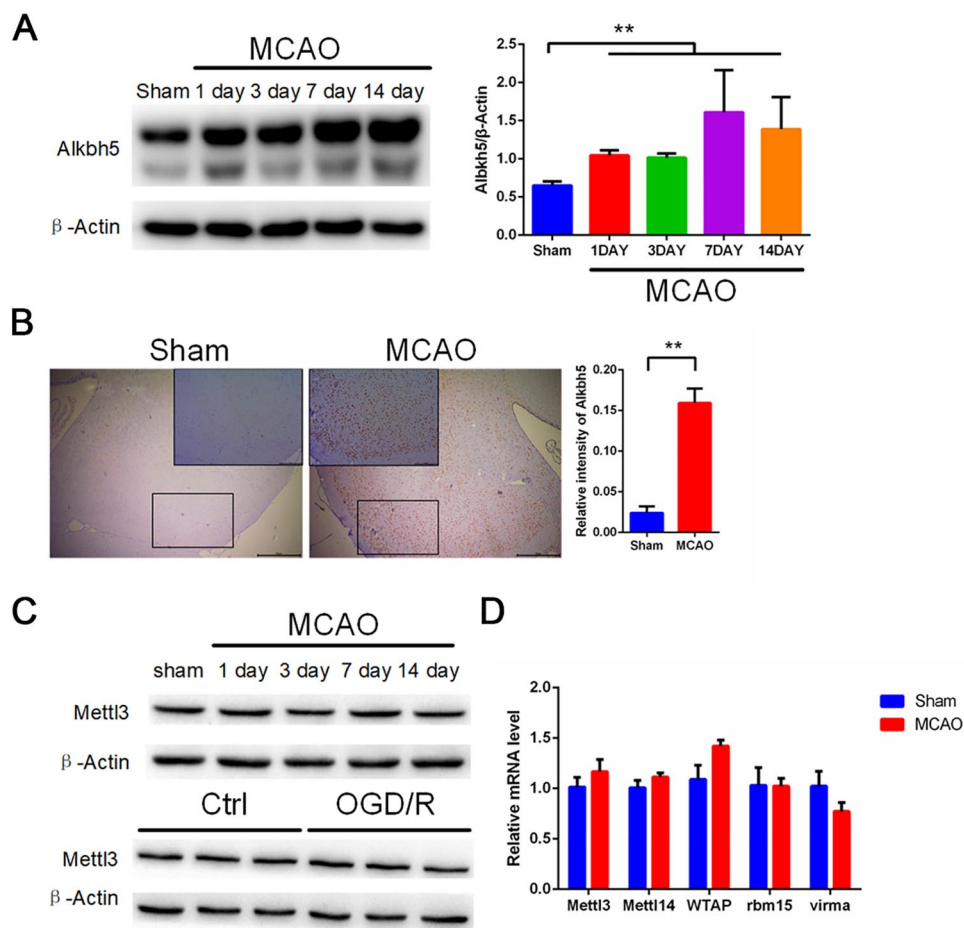


**Figure 3.** MCAO and OGD/R induce elevated levels of Alkbh5 both in rat cerebral cortex and primary cerebral cortical neurons. (A) Representative images of Western blots of MCAO-treated rat cerebral cortex. Alkbh5 levels were determined by Western blot (mean  $\pm$  SEM;  $n \geq 3$ ;  $**p < 0.01$  versus sham). (B) Immunohistochemical results of Alkbh5 in rat cerebral cortex in two indicator groups: tawny staining for Alkbh5 protein and light blue staining for hematoxylin. Scale bar = 50  $\mu$ m, and the small picture scale bar = 20  $\mu$ m. Quantification of Alkbh5 was shown (mean  $\pm$  SEM;  $n = 3$ ;  $**p < 0.01$  versus Sham). (C) Representative images of Western blots of MCAO treated rat cerebral cortex and OGD/R treated primary neurons. Mettl3 levels were determined by Western blot (mean  $\pm$  SEM;  $n = 3$ ;  $ns p > 0.05$  versus Sham or Ctrl). (D) qRT-PCR images of MCAO-treated rat cerebral cortex. Mettl3, Mettl14, WTAP, VIRMA, and RBM15 levels were analyzed by qRT-PCR (mean  $\pm$  SEM;  $n = 3$ ;  $ns p > 0.05$  versus Sham). Ctrl, control; MCAO, middle cerebral artery occlusion; OGD/R, glucose oxygen deprivation/reoxygenation; qRT-PCR, quantitative reverse transcriptase-polymerase chain reaction; SEM, standard error of the mean.

Alkbh5-positive cells after MCAO in rat brain tissue (Figure 3B). Alkbh5 is a demethylase that acts to erase m<sup>6</sup>A. However, we observed a seemingly paradoxical increase in m<sup>6</sup>A modification after I/R as shown in Figure 1. Therefore, we hypothesized that the upregulation of Alkbh5 is compensatory. Furthermore, we did not observe a significant change in *Mettl3* mRNA and protein levels (Figure 3C and Figure S1D) or the level of other demethylases and methyltransferases such as *Mettl14*, *WTAP*, *RBM15*, and *VIRMA* (Figure 3D).

#### *Knockdown of Alkbh5 enhances apoptosis in OGD/R-treated neurons, and overexpression of Fto plays a protective role*

To investigate the role of Alkbh5 in I/R, we used Alkbh5-shRNA to knock down Alkbh5 expression in primary neurons. As shown in Figure S2A, shRNA1 and shRNA2 achieved knockdown efficiencies of more than 70%. We next performed OGD/R treatment on primary cortical neurons with or without Alkbh5 knockdown, and detected apoptosis using flow cytometry. Consistent with



the expected results, Alkbh5 knockdown aggravated neuronal death after OGD/R treatment (Figure 4A). We then found that Alkbh5 knockdown significantly increased cleaved-caspase3 levels after OGD/R treatment (Figure S2B). Furthermore, we tested the activity of primary cortical neurons in the same treatment using the Cell Counting Kit-8 (CCK8) assay. The results were consistent with those from our flow cytometry experiments: Alkbh5 knockdown aggravated the damage caused by OGD/R (Figure 4B). Finally, we performed Hoechst 33342/PI double staining on the same treated cells and found that neuronal death was increased in the Alkbh5-shRNA transduction + OGD/R group relative to the OGD/R group (Figure 4C).

To investigate the role of Fto in I/R, we used Lv-Fto to overexpress Fto in primary neurons. As shown in Figure S2C, Lv-Fto significantly increased the levels of Fto in primary neurons. We next treated primary cortical neurons overexpressing Fto with OGD/R and detected apoptosis using flow cytometry. Consistent with the expected results, overexpression of Fto attenuated neuronal death after OGD/R treatment (Figure 4D). We then found that primary neurons overexpressing Fto had significantly reduced cleaved-caspase3 levels compared with the OGD/R group (Figure S2D). Furthermore, we tested the activity of primary cortical neurons in the same treatment using CCK8. Our findings were consistent with our flow cytometry results: overexpression of Fto alleviated the damage caused by OGD/R (Figure 4E). Finally, we performed Hoechst 33342/PI double staining on the same treated cells and found that neuronal death was reduced in the Lv-Fto transduction + OGD/R group relative to the OGD/R group (Figure 4F).

#### *m<sup>6</sup>A demethylation works through Bcl2*

To investigate the specific mechanism of Alkbh5 in I/R, we determined the expression levels of related proteins in primary cortical neurons with or without Alkbh5 knockdown using Western blot. We found that Alkbh5 knockdown significantly reduced the expression of the apoptosis-related protein Bcl2 in primary neurons, but that the effect of Alkbh5 knockdown on Bax was insignificant (Figure 5A). Previous studies have reported that m<sup>6</sup>A is involved in regulation of the Akt/mTOR signaling pathway and PARP protein

expression. Considering that these proteins play an important role in cerebral ischemia-reperfusion injury, we therefore examined expression of these proteins in primary cortical neurons after Alkbh5 knockdown. Surprisingly, we found that these proteins were not affected by Alkbh5 knockdown in primary cortical neurons (Figure 5B). To further confirm that Bcl2 mRNA is a direct target of m<sup>6</sup>A modification, we obtained the Bcl2 mRNA sequence. Sequence analysis indeed revealed multiple matches of the 5'-RRACH-3'm<sup>6</sup>A consensus sequence in Bcl2 mRNA (Figure 5C). The overexpression of Fto in primary neurons increased the Bcl2 mRNA and protein levels (Figure 5D–E). We examined whether Alkbh5 and Fto affect the stability of Bcl2 mRNA. To this end, primary cortical neurons undergoing Alkbh5 knockdown or Fto overexpression were treated with actinomycin D (Act D) to inhibit RNA elongation. Bcl2 mRNA levels were then examined using qRT-PCR. It was observed that, after treatment with Act D, Bcl2 mRNA was more unstable in primary cortical neurons undergoing Alkbh5 knockdown than in corresponding control cells (Figure 4F). Bcl2 mRNA was more stable in primary cortical neurons overexpressing Fto than in corresponding control cells (Figure 4G).

#### *m<sup>6</sup>A methylation and demethylation drugs play a role in aggravating and reducing cerebral ischemia-reperfusion injury*

In order to investigate the role of m<sup>6</sup>A in I/R, we used Betaine, which is used as a methyl donor to increase global m<sup>6</sup>A levels, and CL, which inhibits the activity of methionine adenosyltransferase, thereby reducing S-adenosylmethionine concentration and decreasing global m<sup>6</sup>A levels, during OGD/R treatment in primary cortical neurons.<sup>14</sup> CCK8 data show that, compared with the OGD/R group, neuronal activity was decreased after adding Betaine (Figure 6C) and increased after adding CL (Figure 6C) following OGD/R treatment in primary cortical neurons. Similarly, we performed Hoechst 33342/PI double staining on the same treated cells. Consistent with CCK8 results, neuronal death was increased in the Betaine group (Figure 6A) and reduced after the addition of CL (Figure 6B) relative to the OGD/R group. Finally, we performed Western blot to quantify the levels of cleaved-caspase3 on the same treated cells. Cleaved-caspase3 was increased in the Betaine group (Figure 6D) and reduced after the

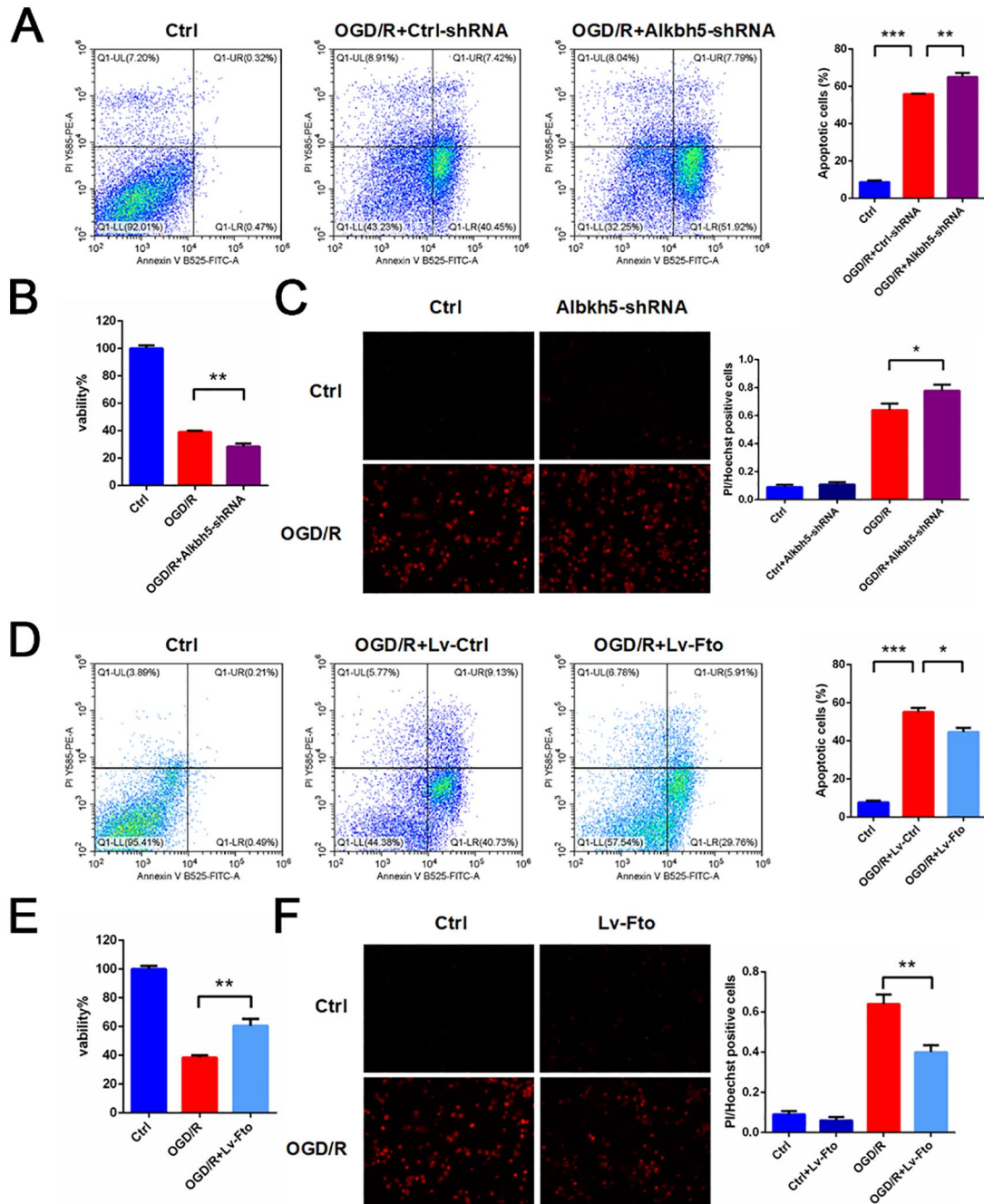


**Figure 4.** Alkbh5 knockdown enhanced OGD/R-treated primary neuronal apoptosis and Fto overexpression attenuated OGD/R-treated primary neuronal apoptosis. (A) Primary neurons were infected with Alkbh5-shRNA and then cultured under OGD/R conditions or normoxia. Apoptosis analysis was performed and representative flow cytometry images are shown. Quantifications of the percentage of apoptotic cells are shown (mean  $\pm$  SEM;  $n=3$ ;  $***p<0.001$  versus Ctrl,  $**p<0.01$  OGD/R + Alkbh5-shRNA versus OGD/R + Ctrl-shRNA). (B) Primary neurons were infected with Alkbh5-shRNA and then cultured under OGD/R conditions or normoxia prior to performing cell activity assays. Quantifications of the percentage of primary neuronal activity are shown (mean  $\pm$  SEM;  $n\geq 8$ ;  $**p<0.01$  OGD/R + Alkbh5-shRNA versus OGD/R). (C) Primary neurons were infected with Alkbh5-shRNA and then cultured under OGD/R conditions or normoxia. Cell death was quantified by microscopy for PI-positive cells. Quantifications of the percentage of dead cells are shown (mean  $\pm$  SEM;  $n=8$ ;  $*p<0.05$  versus OGD/R). (D) Primary neurons were infected with Lv-Fto and then cultured under OGD/R

(Continued)

**Figure 4.** (Continued)

conditions or normoxia. Apoptosis analysis was performed and representative flow cytometry images are shown. Quantifications of the percentage of apoptotic cells are shown (mean  $\pm$  SEM;  $n=3$ ; \*\*\* $p < 0.001$  versus Ctrl, \* $p < 0.05$  OGD/R + Lv-Fto versus OGD/R + Lv-Ctrl). (E) Primary neurons were infected with Lv-Fto and then cultured under OGD/R conditions or normoxia prior to performing cell activity assays. Quantifications of the percentage of primary neuronal activity are shown (mean  $\pm$  SEM;  $n \geq 4$ ; \*\* $p < 0.01$  OGD/R + Lv-Fto versus OGD/R). (F) Primary neurons were infected with Lv-Fto and then cultured under OGD/R conditions or normoxia. Cell death was quantified by microscopy for PI-positive cells. Quantifications of the percentage of dead cells are shown (mean  $\pm$  SEM;  $n=8$ ; \*\* $p < 0.01$  versus OGD/R).  
Ctrl, control; OGD/R, glucose oxygen deprivation/reoxygenation; PI, propidium iodide; SEM, standard error of the mean.

addition of CL (Figure 6E) relative to the OGD/R group.

**Discussion**

In this article, we reveal that *Alkbh5* and *Fto* play important roles in cerebral ischemia-reperfusion injury. We first demonstrated that m<sup>6</sup>A modification levels increased after both neuronal OGD/R treatment and rat MCAO treatment, and that the demethylases *Alkbh5* and *Fto* (but not the methylases *Mettl3* and *Mettl14*) were mainly responsible for abnormal m<sup>6</sup>A modification. We also demonstrated that *Fto* reduction may result in apoptosis in OGD/R-treated neurons, and that compensatory increases in *Alkbh5* protect against the development of ischemia-reperfusion injury. Interestingly, the overexpression of *Fto* alleviated OGD/R-induced neuronal damage, whereas *Alkbh5* knockdown exacerbated OGD/R-induced neuronal damage. These findings demonstrate the treatment potential of the demethylases *Alkbh5* and *Fto* in stroke patients. In addition, we found that *Bcl2* is a key downstream gene regulated by *Alkbh5*. *Alkbh5* knockdown significantly reduced *Bcl2* protein levels, which is probably due to an increase in *Bcl2* methylation levels, leading to degradation of *Bcl2* mRNA. We further show that Betaine and CL, which are methylated and demethylated drugs, respectively, further aggravate or reduce the damage of OGD/R-treated neurons. Besides thrombolysis, there are currently few clinical treatments available for use in stroke patients. Therefore, the regulation of post-transcriptional modifications such as m<sup>6</sup>A, with its rapid onset and reversible nature, could be a new insight into treating stroke.

Although research on m<sup>6</sup>A modification has gradually increased in recent years, there is not much research elucidating the role of m<sup>6</sup>A in cerebral ischemia-reperfusion injury. Previous literature has

pointed out that *Fto*-dependent m<sup>6</sup>A plays an important role in remodeling and repairing cardiac function after heart failure, and is concentrated mainly in the vicinity of the ischemic area.<sup>12</sup> Consistent with their results, we found that *Fto* mRNA and protein levels were significantly reduced in neurons treated with OGD/R. There is therefore reason to believe that cerebral ischemia-reperfusion injury causes corresponding changes in *Fto* expression. Because *Fto* is a dioxygenase that oxidatively demethylates mRNA containing m<sup>6</sup>A,<sup>15</sup> we hypothesized that ischemia or hypoxia would cause a decrease in *Fto* expression and function in cerebral ischemia-reperfusion injury. Because we observed that overexpression of *Fto* significantly reduced neuronal apoptosis after OGD/R treatment, this speculation seems reasonable. Since demethylating m<sup>6</sup>A in single-stranded nuclear RNA is a major function of *Fto*, we attributed the effect of *Fto* alteration directly to altered m<sup>6</sup>A levels in the target transcript. However, we do not rule out *Fto*-dependent N<sup>6</sup>,2'-O-methyladenosine (m<sup>6</sup>Am) demethylation,<sup>16</sup> long non-coding RNA demethylation,<sup>13</sup> or other indirect effects that regulate miRNA expression.

Furthermore, the demethylase *Alkbh5* is a dioxygenase that uses  $\alpha$ -ketoglutarate and O<sub>2</sub> as substrates in the m<sup>6</sup>A demethylation reaction.<sup>17</sup> The scientific fields examining *Alkbh5* are mainly oncology,<sup>18</sup> fertility,<sup>3</sup> cerebellum development,<sup>5</sup> and so on. Recent studies have shown that *Alkbh5* and *Mettl3* act together to regulate hypoxia/reoxygenation of cardiomyocytes by autophagy in an m<sup>6</sup>A-dependent manner.<sup>8</sup> Our investigation also showed that *Alkbh5* mRNA and protein levels were elevated in both OGD/R-treated neurons and MCAO-treated rat cerebral cortex. Consistent with previous studies, hypoxia induced *Alkbh5* expression,<sup>19</sup> but the previous article did not specifically report the function of *Alkbh5*. Considering that *Alkbh5* is a demethylase, however, we

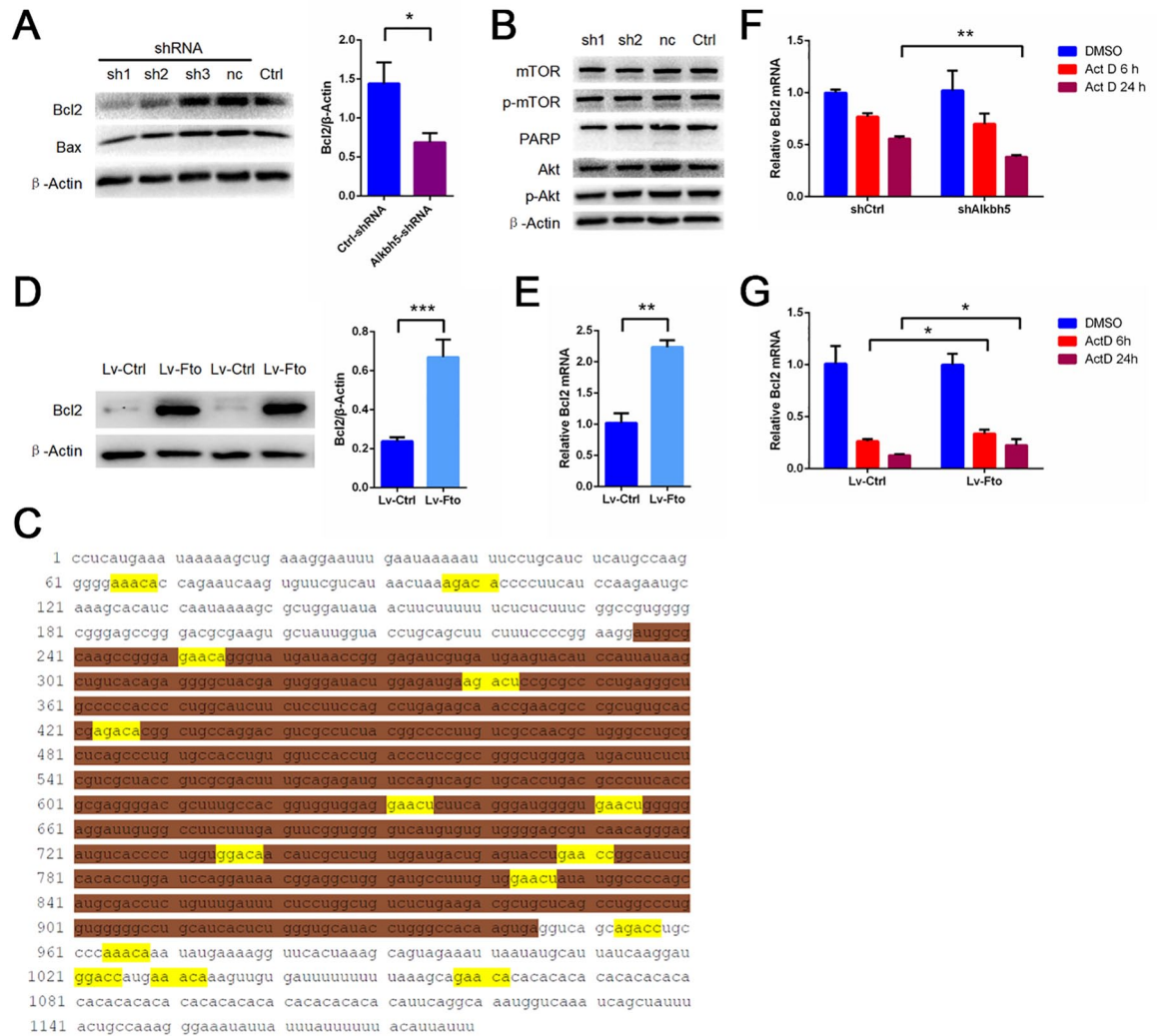


**Figure 5.** Alkbh5 knockdown reduces Bcl2 expression and Fto overexpression increases Bcl2 expression in primary neurons. (A) Representative images of Western blots of primary neurons infected with Alkbh5-shRNA. Bcl2, Bax levels were determined by Western blot (mean ± SEM;  $n \geq 3$ ;  $*p < 0.05$  Ctrl-shRNA versus Alkbh5-shRNA). (B) Representative images of Western blots of primary neurons infected with Alkbh5-shRNA. mTOR, p-mTOR, PARP, Akt, and p-Akt levels were determined by Western blot. (C) Sequence analysis of Bcl2 showed multiple matches with 5'-RRACH-3' (methylated adenosine residues were marked yellow; the first segment of white is Bcl2 3'-UTR, the second segment of brown is Bcl2 CDS, and the third segment of white is Bcl2 5'-UTR) m<sup>6</sup>A consensus sequence. (D) Representative images of Western blots of primary neuron infected with Lv-Fto. Bcl2 levels were determined by Western blot (mean ± SEM;  $n = 6$ ;  $***p < 0.001$  Lv-Fto versus Lv-Ctrl). (E) qRT-PCR images of primary neurons infected with Lv-Fto. Bcl2 levels were analyzed by qRT-PCR (mean ± SEM;  $n = 3$ ;  $**p < 0.01$  Lv-Fto versus Lv-Ctrl). (F) shRNA with or without Alkbh5 was transfected with primary cortical neurons and incubated with 5 μg/ml Act D for a specified time, and then the relative mRNA level of bcl2 was evaluated by qRT-PCR (mean ± SEM;  $n = 3$ ;  $**p < 0.01$ , versus shCtrl Act D 24 h). (G) Lv-Fto was transfected with primary cortical neurons and incubated with 5 μg/ml Act D for a specified time, and then the relative mRNA level of bcl2 was evaluated by qRT-PCR (mean ± SEM;  $n = 3$ ;  $*p < 0.05$ , versus Lv-Ctrl Act D 6 h/24 h). Act D, actinomycin D; CDS, coding sequence; Ctrl, control; m<sup>6</sup>A, N<sup>6</sup>-methyladenosine; SEM, standard error of the mean; shRNA, short-hairpin RNA; UTR, untranslated region.

observed a paradoxical increase in m<sup>6</sup>A levels in Figure 1. We thought that the increase in Alkbh5 expression likely serves to compensate for stress responses in the brain or neuronal ischemia/

hypoxia. Supporting our view, Mathiyalagan *et al.*<sup>12</sup> found a compensatory increase in Alkbh5 expression around the infarct after heart failure. Knocking down Alkbh5 in OGD/R-treated

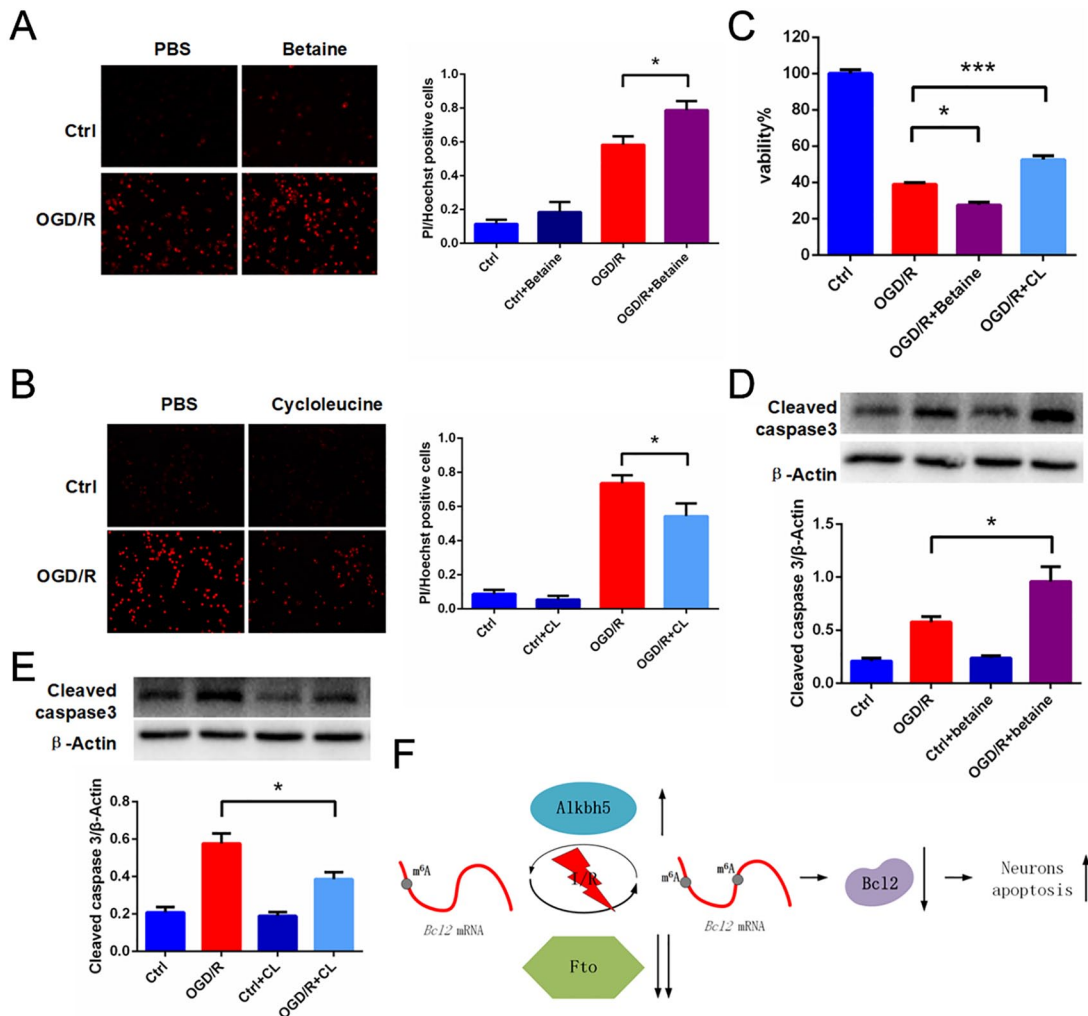


**Figure 6.** Betaine treatment enhanced OGD/R treated primary neuronal death and CL treatment attenuated OGD/R-treated primary neuronal death. [A–C] Primary neurons were treated with 8 mM Betaine or 20 mM CL and then cultured under OGD/R conditions or normoxia. Cell death was quantified by CCK8 assay or by microscopy for PI-positive cells. Quantifications of the percentage of dead cells were shown. (mean  $\pm$  SEM;  $n=6-20$ ; \* $p < 0.05$ , \*\*\* $p < 0.001$  versus OGD/R). [D–E] Representative images of Western blots of primary neuron treated with 8 mM Betaine or 20 mM CL. Cleaved-caspase3 levels were determined by Western blot (mean  $\pm$  SEM;  $n=3$ ; \* $p < 0.05$  versus OGD/R). [F] A proposed model for Alkbh5 and Fto in cerebral ischemia-reperfusion injury. CCK8, Cell Counting Kit-8; CL, cycloleucine; OGD/R, glucose oxygen deprivation/reoxygenation; PI, propidium iodide; SEM, standard error of the mean.

neurons aggravated neuronal damage, indicating that the compensatory rise of Alkbh5 is likely neuroprotective. Interestingly, we performed immunohistochemical staining of MCAO-treated rat brain tissue, we found that Alkbh5 is differentially expressed between the MCAO group and the sham group. Alkbh5 is located mainly in the cg1 area and cg2 area on the caudal of anterior cingulate cortex. These areas are related to attention/perception in the rat, and dysfunction in these

areas has also been implicated in attention deficit hyperactivity disorder and mental illnesses.<sup>20</sup> In addition, stress regulates m<sup>6</sup>A/m in specific brain regions and impaired blood m<sup>6</sup>A/m modification observed in depressed patients.<sup>4</sup> We must think about whether the specific spatial expression of Alkbh5 affects the pathophysiological process of post-stroke depression by affecting local brain methylation. A systematic review and another meta-analysis have concluded that the prevalence

of depression between 1 and 5 years after stroke is estimated to be 30%.<sup>21</sup> Therefore, the hypothesis that Alkbh5-dependent methylation is involved in post-stroke depression deserves further study.

Our results show that Alkbh5 positively regulates Bcl2. We hypothesized that Alkbh5 erased the m<sup>6</sup>A modification on *Bcl2* mRNA, resulting in increased stability of *Bcl2* mRNA. As previously reported, in epithelial ovarian cancer Alkbh5 increases the stability of Bcl2 by modulating m<sup>6</sup>A modification.<sup>22</sup> Bcl2 is known to play a critical role in cerebral ischemic stroke, and our previous results also demonstrate that Bcl2 protein expression is significantly reduced in MCAO-treated rats.<sup>23</sup> We thought that this reduction was most likely due to an increase in Bcl2 methylation levels, causing a decrease in Fto, leading to an increase in Bcl2 degradation. Therefore, we overexpressed Fto in neurons, which significantly increased *Bcl2* mRNA. However, a recent paper reported that Mettl3-mediated dynamic m<sup>6</sup>A modification in human acute myeloid leukemia promoted Bcl2 translation.<sup>24</sup> Therefore, we do not rule out the presence of some mechanisms other than m<sup>6</sup>A modification maintaining mRNA stability in cerebral ischemia-reperfusion injury. In summary, these results indicate that the m<sup>6</sup>A demethylases Alkbh5/Fto are involved, at least in part, in the mechanism of cerebral ischemia-reperfusion injury through m<sup>6</sup>A modification.

In addition, in order to demonstrate that m<sup>6</sup>A modification does play a role in I/R, we used drugs that are reported to promote and inhibit m<sup>6</sup>A modification.<sup>14</sup> Consistent with the expected results, promoting m<sup>6</sup>A modification with Betaine aggravated the damage caused by OGD/R treatment. In contrast, inhibition of m<sup>6</sup>A modification with CL alleviated the damage caused by OGD/R treatment in neurons. However, previous studies have shown that feeding rats betaine protects them from the effects of traumatic brain injury.<sup>25</sup> This is discrepancy probably due to the use of different models and drug concentrations. Thus, we do not completely rule out the biological effects caused by mechanisms other than these two drugs.

In conclusion, we revealed the mechanism of m<sup>6</sup>A modification after cerebral ischemia-reperfusion injury (Figure 6F). I/R-induced neuronal apoptosis was regulated by the m<sup>6</sup>A erasers Alkbh5/Fto.

Therefore, Alkbh5/Fto are potential therapeutic targets for cerebral ischemia-reperfusion injury.

### Acknowledgements

We thank Jianjing Lin for providing the lentiviral envelope and packaging plasmids.

### Author contributions

Conceptualization, Kaiwei Xu and Qinxue Dai; methodology, Kaiwei Xu and Shan Li; software, Qimin Yu; validation, Lu Wang, Feihong Lin, and Chang Kong; formal analysis, Yunchang Mo; investigation, Anqi Zhang; data curation, Sijia Chen; writing—original draft preparation, Kaiwei Xu; writing—review and editing, Meita Felicia Balelang and Junlu Wang; supervision, Junlu Wang; funding acquisition, Junlu Wang.


### Conflict of interest statement

The authors declare that there is no conflict of interest.

### Funding

The authors disclosed receipt of the following financial support for the research, authorship, and/or publication of this article: This work was supported by the National Natural Science Foundation of China, No. 81704180, 81603685, 81573742, 81774109, 81803937; the Natural Science Foundation of Zhejiang Province of China, No. LY19H290008. The major science and technology projects of Wenzhou science and technology bureau No. 2018ZY003.

### ORCID iD

Junlu Wang  <https://orcid.org/0000-0002-7486-2207>

### Supplemental material

Supplemental material for this article is available online.

### References

1. Wang W, Jiang B, Sun H, *et al.* Prevalence, Incidence, and Mortality of Stroke in China: results from a Nationwide Population-Based Survey of 480 687 Adults. *Circulation* 2017; 135: 759–771.
2. Yeo LL, Paliwal P, Teoh HL, *et al.* Timing of recanalization after intravenous thrombolysis and functional outcomes after acute ischemic stroke. *Jama Neurol* 2013; 70: 353–358.

3. Tang C, Klukovich R, Peng H, *et al.* ALKBH5-dependent m<sup>6</sup>A demethylation controls splicing and stability of long 3'-UTR mRNAs in male germ cells. *Proc Natl Acad Sci U S A* 2018; 115: E325–E333.
4. Engel M, Eggert C, Kaplick PM, *et al.* The role of m<sup>6</sup>A/m-RNA methylation in stress response regulation. *Neuron* 2018; 99: 389–403.
5. Ma C, Chang M, Lv H, *et al.* RNA m<sup>6</sup>A methylation participates in regulation of postnatal development of the mouse cerebellum. *Genome Biol* 2018; 19: 68.
6. Shi H, Zhang X, Weng YL, *et al.* m<sup>6</sup>A facilitates hippocampus-dependent learning and memory through YTHDF1. *Nature* 2018; 563: 249–253.
7. Zheng Q, Hou J, Zhou Y, *et al.* The RNA helicase DDX46 inhibits innate immunity by entrapping m<sup>6</sup>A-demethylated antiviral transcripts in the nucleus. *Nat Immunol* 2017; 18: 1094–1103.
8. Song H, Feng X, Zhang H, *et al.* METTL3 and ALKBH5 oppositely regulate m<sup>6</sup>A modification of TFEB mRNA, which dictates the fate of hypoxia/reoxygenation-treated cardiomyocytes. *Autophagy* 2019; 15: 1419–1437.
9. Meyer KD, Saletore Y, Zumbo P, *et al.* Comprehensive analysis of mRNA methylation reveals enrichment in 3' UTRs and near stop codons. *Cell* 2012; 149: 1635–1646.
10. Zhao X, Yang Y, Sun BF, *et al.* FTO-dependent demethylation of N<sup>6</sup>-methyladenosine regulates mRNA splicing and is required for adipogenesis. *Cell Res* 2014; 24: 1403–1419.
11. RajECKA V, SkalICKY T and VanacOVA S. The role of RNA adenosine demethylases in the control of gene expression. *Biochim Biophys Acta Gene Regul Mech* 2019; 1862: 343–355.
12. Mathiyalagan P, Adamiak M, Mayourian J, *et al.* FTO-Dependent N<sup>6</sup>-Methyladenosine regulates cardiac function during remodeling and repair. *Circulation* 2019; 139: 518–532.
13. Zhang S, Zhao BS, Zhou A, *et al.* m<sup>6</sup>A Demethylase ALKBH5 maintains tumorigenicity of glioblastoma stem-like cells by sustaining FOXM1 expression and cell proliferation program. *Cancer Cell* 2017; 31: 591–606.
14. Wang YK, Yu XX, Liu YH, *et al.* Reduced nucleic acid methylation impairs meiotic maturation and developmental potency of pig oocytes. *Theriogenology* 2018; 121: 160–167.
15. Jia G, Fu Y, Zhao X, *et al.* N<sup>6</sup>-methyladenosine in nuclear RNA is a major substrate of the obesity-associated FTO. *Nat Chem Biol* 2011; 7: 885–887.
16. Wei J, Liu F, Lu Z, *et al.* Differential m<sup>6</sup>A, m<sup>6</sup>Am, and m<sup>6</sup>A demethylation mediated by FTO in the cell nucleus and cytoplasm. *Mol Cell* 2018; 71: 973–985.
17. Zheng G, Dahl JA, Niu Y, *et al.* ALKBH5 is a mammalian RNA demethylase that impacts RNA metabolism and mouse fertility. *Mol Cell* 2013; 49: 18–29.
18. Zhang C, Samanta D, Lu H, *et al.* Hypoxia induces the breast cancer stem cell phenotype by HIF-dependent and ALKBH5-mediated m<sup>6</sup>A-demethylation of NANOG mRNA. *Proc Natl Acad Sci U S A* 2016; 113: E2047–E2056.
19. Thalhammer A, Bencokova Z, Poole R, *et al.* Human AlkB homologue 5 is a nuclear 2-oxoglutarate dependent oxygenase and a direct target of hypoxia-inducible factor 1alpha (HIF-1alpha). *Plos One* 2011; 6: e16210.
20. Ash ES, Heal DJ and Clare SS. Contrasting changes in extracellular dopamine and glutamate along the rostrocaudal axis of the anterior cingulate cortex of the rat following an acute d-amphetamine or dopamine challenge. *Neuropharmacology* 2014; 87: 180–187.
21. Ferro JM, Caeiro L and Figueira ML. Neuropsychiatric sequelae of stroke. *Nat Rev Neurol* 2016; 12: 269–280.
22. Zhu H, Gan X, Jiang X, *et al.* ALKBH5 inhibited autophagy of epithelial ovarian cancer through miR-7 and BCL-2. *J Exp Clin Cancer Res* 2019; 38: 163.
23. He X, Mo Y, Geng W, *et al.* Role of Wnt/beta-catenin in the tolerance to focal cerebral ischemia induced by electroacupuncture pretreatment. *Neurochem Int* 2016; 97: 124–132.
24. Vu LP, Pickering BF, Cheng Y, *et al.* The N<sup>6</sup>-methyladenosine (m<sup>6</sup>A)-forming enzyme METTL3 controls myeloid differentiation of normal hematopoietic and leukemia cells. *Nat Med* 2017; 23: 1369–1376.
25. Ataizi S, Ozkoc M, Kanbak G, *et al.* A possible protective role of betain and omega-3 supplementation in traumatic brain injury. *Ann Ital Chir* 2019; 90: 174–181.
26. Yousefzadeh MJ, Wyatt DW, Takata K, *et al.* Mechanism of suppression of chromosomal instability by DNA polymerase POLQ. *Plos Genet* 2014; 10: e1004654.